

# A New Series of Photoactivatable and Iodinatable Linear Vasopressin Antagonists<sup>†</sup>

Eric Carnazzi, André Aumelas, Claude Barberis,<sup>†</sup> Gilles Guillon,<sup>†</sup> and René Seyer\*

UPR 9023 CNRS, Mécanismes Moléculaires des Communications Cellulaires, and U401 INSERM, CCIPE, rue de la Cardonille F-34094 Montpellier Cedex 5, France

Received December 29, 1993\*

A series of new linear photoactivatable and iodinated antagonists of the neuropeptidic hormone vasopressin was designed and synthesized by a combination of PyBOP-mediated Boc/solid-phase peptide synthesis and solution synthesis approaches. These were based on modifications of a previously reported potent and selective antagonist of the vasopressor response ( $V_{1a}$  receptor) to [arginine]vasopressin, phenylacetyl-D-Tyr(Me)-Phe-Gln-Asn-Arg-Pro-Arg-Tyr-NH<sub>2</sub>. (Azidophenyl)alkyl substitutions, of the general structure N<sub>3</sub>-C<sub>6</sub>H<sub>4</sub>(CH<sub>2</sub>)<sub>n</sub>CO ( $n = 0, 1, 2, \text{ or } 3$ ), were employed in position 1. The seven new analogues are 4-N<sub>3</sub>-C<sub>6</sub>H<sub>4</sub>CO-D-Tyr(Me)-Phe-Gln-Asn-Arg-Pro-Arg-Tyr-NH<sub>2</sub> (3), 3-N<sub>3</sub>-C<sub>6</sub>H<sub>4</sub>CO-D-Tyr(Me)-Phe-Gln-Asn-Arg-Pro-Arg-Tyr-NH<sub>2</sub> (12), 4-N<sub>3</sub>-C<sub>6</sub>H<sub>4</sub>CH<sub>2</sub>CO-D-Tyr(Me)-Phe-Gln-Asn-Arg-Pro-Arg-Tyr-NH<sub>2</sub> (13), 3-N<sub>3</sub>-C<sub>6</sub>H<sub>4</sub>CH<sub>2</sub>CO-D-Tyr(Me)-Phe-Gln-Asn-Arg-Pro-Arg-Tyr-NH<sub>2</sub> (14), 4-N<sub>3</sub>-C<sub>6</sub>H<sub>4</sub>(CH<sub>2</sub>)<sub>2</sub>CO-D-Tyr(Me)-Phe-Gln-Asn-Arg-Pro-Arg-Tyr-NH<sub>2</sub> (15), 3-N<sub>3</sub>-C<sub>6</sub>H<sub>4</sub>(CH<sub>2</sub>)<sub>2</sub>CO-D-Tyr(Me)-Phe-Gln-Asn-Arg-Pro-Arg-Tyr-NH<sub>2</sub> (16), 4-N<sub>3</sub>-C<sub>6</sub>H<sub>4</sub>(CH<sub>2</sub>)<sub>3</sub>CO-D-Tyr(Me)-Phe-Gln-Asn-Arg-Pro-Arg-Tyr-NH<sub>2</sub> (17). All analogues were tested for their affinity of the rat hepatic  $V_{1a}$  receptor. Analogues 3 and 12 have a low affinity ( $K_i \approx 20$  nM) and analogues 13-17 show a high affinity ( $K_i$  between 0.04 and 0.3 nM). The affinity values appear to be mainly a function of the alkyl chain length and to a lesser extent of the meta or para position of the azido group on the aromatic ring. Analogues 13-17 were iodinated on the Tyr-9 residue, giving compounds 18-22. All these five iodinated derivatives exhibited  $K_i$  values of 0.2-1 nM for rat liver membranes. Their affinities for oxytocin and renal  $V_2$  vasopressin receptors were much lower. Moreover, all analogues completely antagonized the vasopressin-stimulated inositol phosphates production in WRK<sub>1</sub> cells and were devoided of any agonistic potency. Preliminary covalent binding studies showed improved covalent yields as compared to any previously reported results. They are very promising candidates as potential high-affinity, highly selective, photosensitive ligands for the  $V_{1a}$  receptor. They could serve as useful pharmacological tools for studies on the vasopressin binding site.

## Introduction

Vasopressin (VP) is a neurohypophyseal nonapeptidic hormone having a disulfide bridge in positions 1,6. This neuropeptide regulates a wide range of cellular functions by interacting with two classes of receptors,  $V_1$  and  $V_2$ . The  $V_1$  receptors are functionally coupled to the phosphatidylinositol-4,5-bisphosphate phospholipase C. They have been divided into two subtypes. The  $V_{1a}$  subtype is found in liver, vascular smooth muscles, platelets, central nervous system, and many other peripheral tissues. They regulate numerous effects such as glycogenolysis, vasoconstriction, platelet aggregation, and neurotransmission. The  $V_{1b}$  subtype is found in the adenohipophysis. It has

a very low affinity for vasopressin antagonists and it is involved in the multifunctional regulation of corticotropin release. The  $V_2$  receptors are the renal adenylate cyclase-coupled receptors involved in the antidiuretic effect of vasopressin.

In order to study the function and the pharmacology of these receptors, much work has been done in the synthesis of radiolabeled AVP analogues with enhanced affinity and specificity for both agonists and antagonists. Successive improvements were obtained with the following modifications: (i) the elimination of the *N*-terminal amino group and the introduction of bulky and hydrophobic desamino groups at position 1 (increase in affinity),<sup>1</sup> (ii) the introduction of a second Tyr-residue at position 9 and its selective iodination (Tyr-2 iodination being prevented by *O*-alkylation), and (iii) the discovery that a cyclic structure was not a requirement for receptor recognition.<sup>2</sup> These modifications led to the synthesis of a radioiodinated vasopressin antagonist specific for  $V_{1a}$  vasopressin receptors.<sup>3</sup> It is a useful tool for studying vasopressin receptor localization and characterization. Nevertheless, the biochemical study of these membrane receptors is still limited by their scarcity, hydrophobicity, and fragility. In particular, a problem is that denaturation of the receptor during its isolation by solubilization caused a loss in binding and activity. Therefore several studies have been directed to the use of cross-linking reagents<sup>4</sup> or photoreactive analogues which can be covalently linked to the receptor.<sup>5,6</sup> Jointly used with a radiolabeled isotope, a biotinyl group,<sup>7</sup> or a fluorescent group,<sup>8</sup> the obtained peptide probes would

<sup>†</sup> Abbreviations according to the IUPAC-IUB Commission (*Eur. J. Biochem.* 1984, 138, 9-37) are used throughout. In addition, the following abbreviations are used: AVP, [arginine]vasopressin; Boc, *tert*-butyloxy-carbonyl; BOP, (1*H*-1,2,3-benzotriazol-1-yl-oxy)tris(dimethylamino)phosphonium hexafluorophosphate; BSA, bovin serum albumin; Bz, benzoyl; Dcb, 2,6-dichlorobenzyl; DCM, dichloromethane; DIEA, diisopropylethylamine; DMF, dimethylformamide; Me<sub>2</sub>SO, dimethyl sulfoxide; D-Tyr(Me), *O*-methyl-D-tyrosine;  $\epsilon$ , molar extinction coefficient; FAB-MS, fast atom bombardment mass spectrometry; HOBt, hydroxybenzotriazole; HPLC, high-performance liquid chromatography; *J*, coupling constant;  $K_d$ , dissociation constant;  $K_i$ , inhibition constant;  $K_{i,act}$ , inhibition constant of vasopressin-induced inositol phosphates accumulation; MBHA, methylbenzhydrylamine resin; NOESY, nuclear Overhauser spectroscopy; PyBOP, (benzotriazolyl)oxytripyrrolidinophosphonium hexafluorophosphate; Phaa, phenylacetyl; Phba, phenylbutyryl; Phpa, phenylpropionyl; RP, reverse phase; TFA, trifluoroacetic acid; Tris (trishydroxymethyl)aminomethane; TOCSY, total correlation spectroscopy; Tos, tosyl;  $V_{1a}$ ,  $V_{1b}$ ,  $V_2$ , vasopressin receptor subtypes; VP, vasopressin; VT, vasotocin; Xan, xanthyl.

\* Author to whom correspondence should be addressed.

<sup>†</sup> U401 INSERM.

• Abstract published in *Advance ACS Abstracts*, May 1, 1994.

allow a good detection of the receptor, even in its denaturated form.

Despite numerous attempts, there are no efficient photoactivatable analogues currently available for vasopressin receptors. Recently, Barbeau *et al.* reported an analogue to have an affinity in the nanomolar range, but its covalent yield was not stated.<sup>9</sup> Therefore, we were interested in synthesizing new efficient photoactivatable linear probes to explore the amino acid environment of the vasopressin binding site. In order to design rational probes, we took into account several important observations: (i) The *N*-terminal sequence of vasopressin is important for both binding to the receptor and to neurophysin,<sup>10</sup> its protein carrier. However, if the terminal protonated amino group ( $\text{NH}_3^+$ ) is structurally necessary for the binding of the peptide to neurophysin, Manning *et al.* described that hydrophobic bulky desamino groups can increase the affinity of the probe for the receptor.<sup>1,11</sup> On the basis of results obtained from past studies, we considered that these groups could fit into a structurally defined subsite of the receptor binding site which has a particular affinity for hydrophobic groups. Therefore, we speculated that high-affinity binding could be partly the result of specific interactions between the constitutive residues of the subsite and the *N*-terminal section of the probe. (ii) As higher covalent binding yields would probably be obtained with the closer proximity of the photoreactive group to the subsite contour, we decided to study antagonists containing a photoreactive group specifically at position 1 because previous work established that a photoactivatable group at positions 3, 4, 8, or 9 gave very low covalent yields (reviewed in ref 9). (iii) Among several photoreactive groups, the azido group was selected because its lipophilicity has been well-established by RP-HPLC and partition data. (iv) Manning reported that Phaa-D-Tyr(Me)-Phe-Gln-Asn-Arg-Pro-Arg-Tyr-NH<sub>2</sub> antagonist (with Phaa for phenylacetyl) exhibited a high affinity which was still preserved after iodination of the Tyr-9; we therefore selected this peptide sequence as the basis of this present work with the serious hope that our modifications will not affect their relative biological activities. Furthermore, the use of antagonists in the receptor labeling has many advantages such as slow binding reversibility with the receptor, reduced internalization of the probe-receptor complex,<sup>12,13</sup> and no inactivation of the transduction mechanism (G protein). Considering all these data, a range of analogues was prepared. Their chemical structures, affinities for various vasopressin receptors, ability to covalently link vasopressin receptor, and agonistic or antagonistic properties were determined by two-dimensional NMR, bindings experiments, photoactivation of analogue-receptor complexes, and influence on WRK<sub>1</sub> cell inositol phosphates accumulation, respectively.

## Results and Discussion

A series of vasopressin analogues were synthesized of which the general formula is given in Figure 1. Several azido aromatic acids were used with different chain lengths ( $n = 0, 1, 2, \text{ or } 3$ ) and with different positions of the azido group (para, meta) in order to find the best structure giving high covalent linkage yield (see Table 3). In the case of efficient photoactivation, such probes would be of great interest in a close "mapping" of the receptor antagonist binding site by their covalent linking to various residues of the pocket.

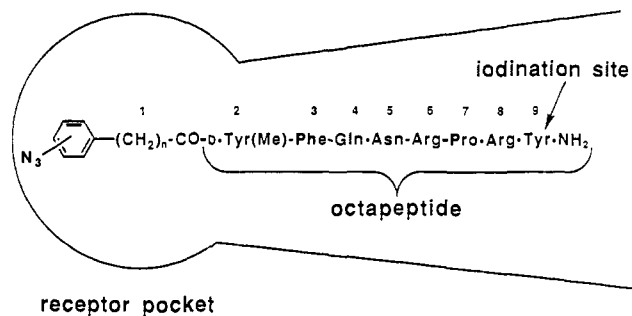


**Figure 1.** Design of new photoactivatable analogues of vasopressin. Proposed receptor-ligand model based on the hypothesis that the receptor pocket has a high affinity for analogues having a hydrophobic "head". In order to examine the effect due to the structure of this "head" on the affinity, peptide probes were designed containing variable methylene spacer units ( $n = 0, 1, 2, \text{ or } 3$ ) and the azido group in the *m*- or *p*-position of the aromatic ring.

All peptides were prepared by Boc solid-phase peptide synthesis which used PyBOP<sup>14</sup> as the coupling reagent. The 3-(3- and 3-(4-aminophenyl)propionic acids were obtained by hydrogenation of the commercially available 3-nitrocinnamic (3-NO<sub>2</sub>-C<sub>6</sub>H<sub>4</sub>CH=CHCOOH) and 4-aminocinnamic acids (4-NH<sub>2</sub>-C<sub>6</sub>H<sub>4</sub>CH=CHCOOH), respectively. The 3- and 4-aminobenzoic, 3- and 4-aminophenylacetic, and (4-aminophenyl)butyric acids were commercially available. All couplings, hydrogenations, azidations,<sup>15</sup> and iodinations were monitored by HPLC using dual UV wavelength detection at 214 and 254 nm.<sup>16</sup> Derivatives 13–17 were iodinated using ICl in methanol or radioiodinated conveniently just before use. The purity of all peptides was assessed by RP-HPLC and their structures confirmed by FAB-MS. Since octapeptide 1 was an important and common peptide segment of all azido peptides, its chemical structure was confirmed by two-dimensional NMR with all expected spin systems being identified in the TOCSY experiment (Figure 2a).<sup>17</sup> The  $\beta\beta'$  chemical shifts of these different systems are characteristic of each amino acid family, and assignments were mainly performed using sequential NOEs ( $\alpha\text{H}_i\text{-HN}_{i+1}$ , arrows in the Figure 2b, and  $\text{HN}_i\text{-HN}_{i+1}$ ).<sup>18</sup> In this manner, the signals of the two Arg residues were assigned and the peptide sequence confirmed. The side-chain amide protons were observed but not assigned. All chemical shifts are presented in Table 1. The obtained NMR data ( $^3J_{\text{HN-C}_\alpha\text{H}}$  coupling constants and NOEs) indicate that the octapeptide has an extended conformation. The observation of a strong NOE between the Arg-5 H <sub>$\alpha$</sub>  proton with the Pro-6 H <sub>$\beta$</sub> -H <sub>$\beta'$</sub>  protons suggests a trans conformation for the Arg-5/Pro-6 amide bond.

**Affinities of Vasopressin Analogues on the Different Vasopressin Receptor Subtypes.** The affinities of compounds 3 and 12–22 were determined on purified plasma membranes preparations from rat liver<sup>19</sup> exhibiting the V<sub>1a</sub> vasopressin receptor subtype. The affinities of compounds 18–22 were also determined on membrane preparation from rat renal medullary<sup>20</sup> and rat mammary gland<sup>21</sup> exhibiting the V<sub>2</sub> vasopressin receptor subtype and the oxytocin receptor, respectively.

Two techniques were used to measure the vasopressin analogues affinities: (1) concentration-dependent binding inhibition using specific radiolabeled vasopressin or oxytocin probes characterized earlier and (2) concentration-dependent binding experiments using the radioiodinated vasopressin analogues.

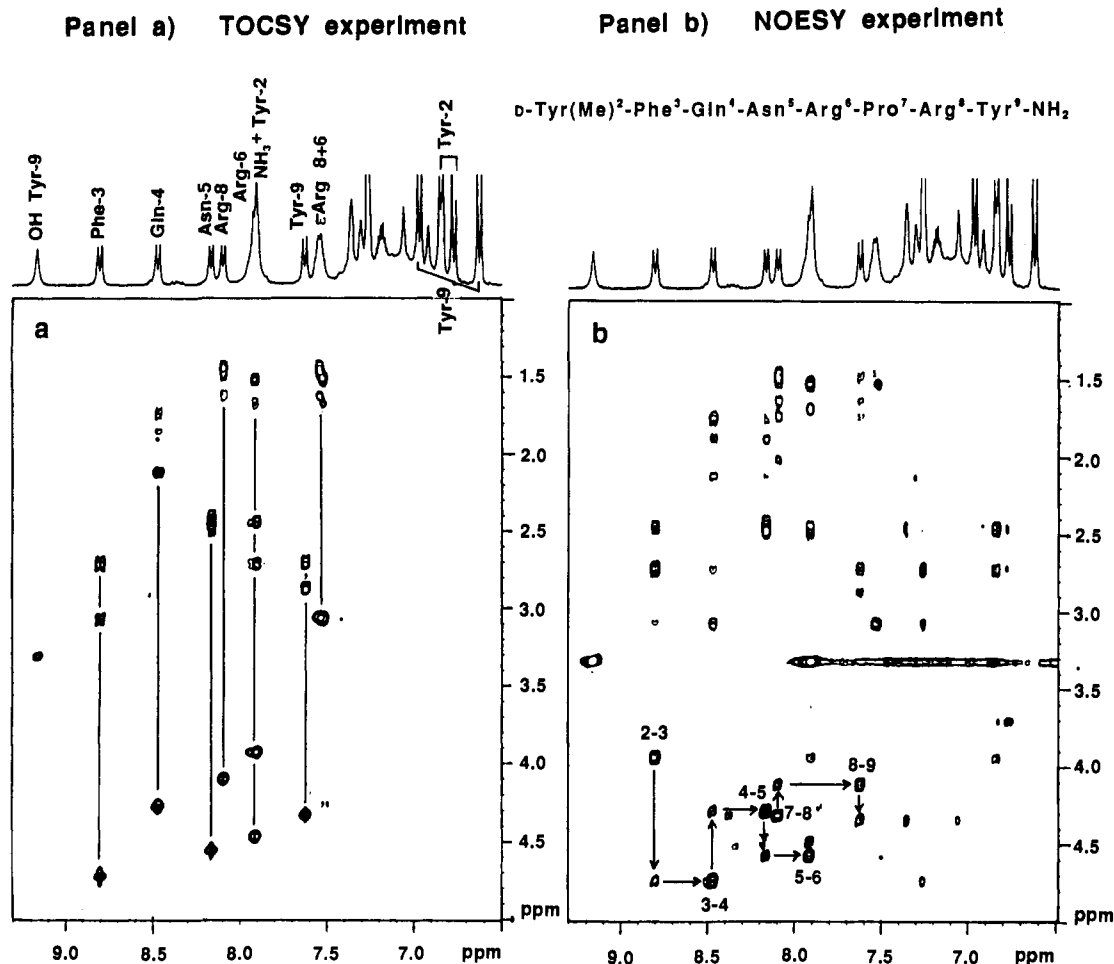


**Figure 2.** <sup>1</sup>H NMR spectrum of octapeptide 1 showing the HN-aliphatic region of the spectrum. The residues are numbered as in vasopressin. Panel a shows the TOCSY spectrum. All spin systems are identified and assignments are indicated on the 1D spectrum. Panel b shows the same region of the NOESY spectrum recorded with a mixing time of 300 ms showing the  $\alpha$ H<sub>T</sub>-HN<sub>T+1</sub> sequential cross-peaks. They are labeled by two numbers. For example 2-3 means a NOE between the  $\alpha$  proton of residue 2 with the amide proton of residue 3. The two Arg were assigned in this way.

**Table 1.** Proton Resonance Assignments of the Octapeptide H-Tyr<sup>2</sup>-Phe<sup>3</sup>-Gln<sup>4</sup>-Asn<sup>5</sup>-Arg<sup>6</sup>-Pro<sup>7</sup>-Arg<sup>8</sup>-Tyr<sup>9</sup>-NH<sub>2</sub> in [2H]<sub>6</sub>Me<sub>2</sub>SO at 305 K<sup>a</sup>

residue	NH (ppm)	<sup>3</sup> J <sub>HN-C<math>\alpha</math>H</sub> (Hz)	H <sub><math>\alpha</math></sub> (ppm)	H <sub><math>\beta,\beta'</math></sub> (ppm)	others (ppm)
Tyr <sup>2</sup> (Me)	7.91		3.94	2.73	H <sub><math>\beta,\beta'</math></sub> , 6.85; H <sub><math>\epsilon,\epsilon'</math></sub> , 6.77
Phe <sup>3</sup>	8.80	8.6	4.74	2.46 3.07 2.71	OMe, 3.70 H <sub><math>\beta,\beta'</math></sub> , H <sub><math>\epsilon,\epsilon'</math></sub> , H <sub>T</sub> ; 7.3-7.0
Gln <sup>4</sup>	8.47	7.8	4.28	1.86 1.74	H <sub><math>\gamma,\gamma'</math></sub> , 2.13; N <sub><math>\epsilon,\epsilon'</math></sub> H <sub>2</sub> <sup>b</sup>
Asn <sup>5</sup>	8.17	7.3	4.58	2.44	N <sub><math>\gamma,\gamma'</math></sub> H <sub>2</sub> <sup>b</sup>
Arg <sup>6</sup>	7.92		4.48	1.69 1.53	H <sub><math>\gamma,\gamma'</math></sub> , 1.52; H <sub><math>\beta,\beta'</math></sub> , 3.09 N <sub><math>\epsilon,\epsilon'</math></sub> H <sub>2</sub> , 7.54
Pro <sup>7</sup>			4.31	2.01 1.76	H <sub><math>\gamma,\gamma'</math></sub> , 1.86; H <sub><math>\beta,\beta'</math></sub> , 3.62, 3.50
Arg <sup>8</sup>	8.10	7.4	4.12	1.65 1.51	H <sub><math>\gamma,\gamma'</math></sub> , 1.47; H <sub><math>\beta,\beta'</math></sub> , 3.09 N <sub><math>\epsilon,\epsilon'</math></sub> H <sub>2</sub> , 7.54
Tyr <sup>9</sup>	7.63	7.9	4.34	2.88 (4.9 <sup>c</sup> ) 2.70 (13.9 <sup>d</sup> )	H <sub><math>\beta,\beta'</math></sub> , 6.97; H <sub><math>\epsilon,\epsilon'</math></sub> , 6.63 OH, 9.16; NH <sub>2</sub> <sup>b</sup>

<sup>a</sup> The residual signal of [2H]<sub>6</sub>Me<sub>2</sub>SO was taken as chemical shifts reference (2.5 ppm). <sup>3</sup>J<sub>HN-C $\alpha$ H</sub> coupling constants are reported. <sup>b</sup> The three NH<sub>2</sub> amide proton pairs are observed at 7.37-6.92; 7.36-7.06 and 7.31-6.85 ppm but not assigned. <sup>c</sup> <sup>3</sup>J <sub>$\alpha\beta$</sub> . <sup>d</sup> <sup>2</sup>J <sub>$\beta\beta$</sub> .

Figure 3 illustrates the concentration-displacement curves obtained for derivatives 3 and 12-22 on rat liver membranes using [<sup>125</sup>I]Phaa-D-Tyr(Me)-Phe-Gln-Asn-Arg-Pro-Arg-Tyr-NH<sub>2</sub> as the labeled tracer.<sup>3</sup> All analogues tested were able to fully inhibit the [<sup>125</sup>I]Phaa-D-Tyr(Me)-Phe-Gln-Asn-Arg-Pro-Arg-Tyr-NH<sub>2</sub> specific binding, suggesting that they compete with the same binding sites labeled with the radioiodinated analogue. Moreover, the concentration-displacement curves exhibit a profile similar to each other. The Hill coefficient calculated from these

experiments varied from 1.0 to 1.2, suggesting a Michaelian competition at the binding site level. The affinities of each analogue were determined as described in Experimental Section and the statistical values are summarized in Tables 2 and 3.

These data show that, except for compounds 3 and 12, all the noniodinated derivatives had a good affinity ( $K_1$  in a range of 0.04 and 0.3 nM) and highlighted the importance of the alkyl chain length. The low affinities of analogues 3 and 12 ( $K_1$  values of 20 and 17.8 nM, respectively) are

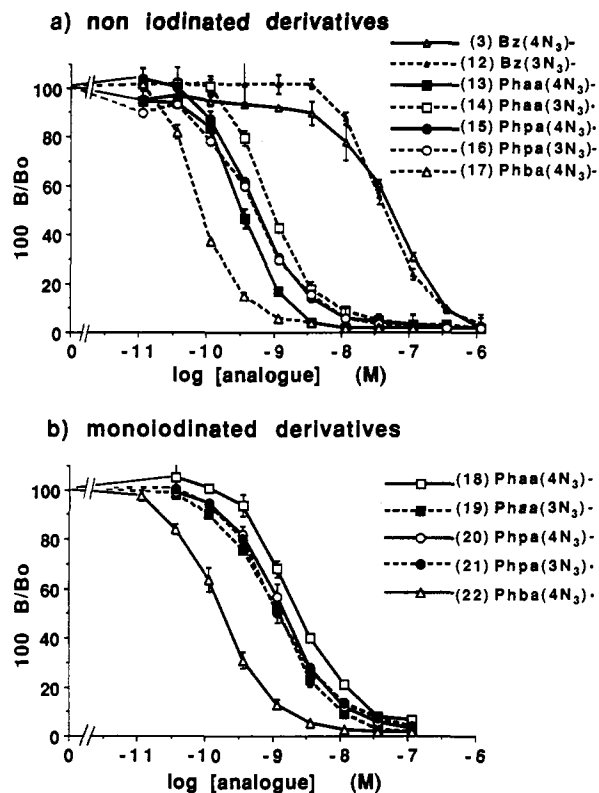


**Figure 3.** Determination of vasopressin analogue affinities by concentration-displacement binding experiments. Rat liver membranes were incubated for 45 min in the dark at 30 °C in the presence of increasing amounts of unlabeled peptides ( $10^{-11}$  to  $10^{-7}$  or  $10^{-6}$  M) and  $60 \cdot 10^{-12}$  M of [ $^{125}$ I]Phaa-D-Tyr(Me)-Phe-Gln-Asn-Arg-Pro-Arg-Tyr-NH<sub>2</sub> (linear AVP antagonist). Values of specific binding measured in the presence of unlabeled peptides ( $B$ ) were expressed as a fraction of the specific binding ( $B_0$ ) measured in the absence of competitor ( $B_0 = 597 \pm 73$  fmol/mg of protein). The apparent dissociation constants ( $K_i$ ) for the nonlabeled peptides were calculated by using the following relation:  $K_i = IC_{50} \times K_{d \cdot H} / (K_{d \cdot H} + [^*H])$  in which  $IC_{50}$  is the concentration of unlabeled peptide leading to half-maximal inhibition of labeled antagonist specific binding,  $K_{d \cdot H}$  (0.06 nM) is the dissociation constant at the equilibrium of iodinated linear AVP antagonist, and [ $^*H$ ] is the concentration of the iodinated linear AVP antagonist in the incubation medium. Panel a shows representative concentration-displacement curves of compounds 3 and 12–17. Panel b shows representative concentration-displacement curves of compounds 18–22. Results are the mean  $\pm$  SE of triplicate determinations from a single experiment representative of two to seven experiments. When no error bar is shown, it is comprised within the symbols.

**Table 2.** Chemical and Biochemical Data of the Noniodinated Derivatives (Analogues 3 and 12–17)

compd	position moiety		formula (without TFA)	FAB-MS (M + 1)	$K_i^a$ (nM)
	1	9			
3	Bz(4-N <sub>3</sub> )	Tyr	C <sub>61</sub> H <sub>80</sub> O <sub>13</sub> N <sub>20</sub>	1301	20.0 (2)
12	Bz(3-N <sub>3</sub> )	Tyr	C <sub>61</sub> H <sub>80</sub> O <sub>13</sub> N <sub>20</sub>	1301	17.8 (2)
13	Phaa(4-N <sub>3</sub> )	Tyr	C <sub>62</sub> H <sub>82</sub> O <sub>13</sub> N <sub>20</sub>	1315	0.12 (2)
14	Phaa(3-N <sub>3</sub> )	Tyr	C <sub>62</sub> H <sub>82</sub> O <sub>13</sub> N <sub>20</sub>	1315	0.31 (2)
15	Phpa(4-N <sub>3</sub> )	Tyr	C <sub>63</sub> H <sub>84</sub> O <sub>13</sub> N <sub>20</sub>	1329	0.20 (2)
16	Phpa(3-N <sub>3</sub> )	Tyr	C <sub>63</sub> H <sub>84</sub> O <sub>13</sub> N <sub>20</sub>	1329	0.16 (2)
17	Phba(4-N <sub>3</sub> )	Tyr	C <sub>64</sub> H <sub>86</sub> O <sub>13</sub> N <sub>20</sub>	1343	0.04 (3)

<sup>a</sup>  $K_i$ : inhibition constants determined from competitive binding experiments performed on rat liver membranes ( $V_{1a}$  receptor subtype). The results are the mean values of triplicate determination obtained from the number of experiments indicated in parentheses.

attributed to the rigidity of the azidophenyl moiety due to its amide linkage with the peptide. In contrast, the higher affinities of the Phaa, Phpa, and Phba derivatives

(13–17) are attributed to the additional one, two, and three methylene units (between the azidophenyl moiety and the amide linkage) increasing the flexibility of the azidophenyl moiety with respect to the peptide backbone. As the affinities of the Phaa and Phpa derivatives were similar but lower than that of Phba, we therefore considered that, for these series, the alkyl chain length is critical for efficient probe-receptor interaction and that, in this case, the one, two, and three methylene alkyl chain lengths can be accommodated by the binding site (compare compounds 13 and 14 with 15 and 16 and with 17, Table 2). In addition, the minor difference in values observed for compounds 13 and 14 indicates that the position of the azido moiety (para or meta, Table 2) on the phenyl group had no influence on the affinity, the  $K_i$  only changing from 0.1 to 0.3 nM, respectively. Since the iodination of the Tyr-9 residue only caused a small decrease in the affinity (see Table 3), we hoped that these analogues could be potential candidates for the  $^{125}$ I radiolabeling of the vasopressin receptor in high covalent yields. Hence, it is plausible that variations in both the alkyl chain length of the azidophenylalkyl group and the aromatic position of the photo-reactive group will show much promise for obtaining good covalent yields as well as for the complete mapping of the receptor binding site. The only analogue described to date with an azido group in the *N*-terminal position had a low affinity ( $K_d = 75.4$  nM) and was not iodinated due to a lack of a suitable site.<sup>9</sup>

Vasopressin analogues 18 and 20–22 were also prepared in their  $^{125}$ I radiolabeled form, as described in Experimental Section, and their affinities determined directly by testing their ability to interact with specific receptors. Figure 4 shows a typical representation of a Scatchard plot obtained with analogue 21 on rat liver membranes. As earlier described with [ $^3$ H]AVP or with [ $^{125}$ I]Phaa-D-Tyr(Me)-Phe-Gln-Asn-Arg-Pro-Arg-Tyr-NH<sub>2</sub>, the Scatchard representation of the concentration binding experiments was linear, suggesting the interaction of labeled analogues with a single class of specific vasopressin receptors. The affinity obtained by this technique (0.054 nM) was statistically similar to the one determined by a concentration-displacement experiment. Similar experiments were also performed with analogues 18, 20, and 22 and gave similar results (see Table 3).

The affinities of analogues 18–22 for the rat renal vasopressin receptor ( $V_2$  subtype) and for the rat mammary gland oxytocin receptor were also determined by concentration-displacement experiments in order to study their specificity. Results are summarized in Table 3. Analogues 19 and 21 were rather selective between  $V_{1a}$  and  $V_2$  vasopressin receptor subtypes but exhibited similar affinities for  $V_{1a}$  vasopressin and oxytocin receptors. In contrast, analogue 20 exhibited similar affinities for  $V_{1a}$  and  $V_2$  receptor subtypes and discriminated quite well  $V_{1a}$  vasopressin and oxytocin receptors. Finally, analogue 22 and, to a lesser extent, analogue 18 exhibited both high affinity and specificity for the  $V_{1a}$  vasopressin receptor subtype (0.18–0.59 nM).

Therefore, if the differences of the affinity of analogues 18–22 (and previously of analogues 3 and 12–17) for the  $V_{1a}$  vasopressin receptor subtype is mainly due to the alkyl chain length, this is not the case for other receptor subtypes. As a matter of fact, compounds 18–21 have different affinities for the oxytocin receptor that we explain by the position of the azido group. From these observations, it

**Table 3.** Chemical and Biochemical Data of the Iodinated Derivatives (Analogues 18–22)

	18	19	20	21	22
position moiety					
1	Phaa(4-N <sub>3</sub> )	Phaa(3-N <sub>3</sub> )	Phpa(4-N <sub>3</sub> )	Phpa(3-N <sub>3</sub> )	Phba(4-N <sub>3</sub> )
9	Tyr(3-I)	Tyr(3-I)	Tyr(3-I)	Tyr(3-I)	Tyr(3-I)
formula (without TFA)	C <sub>62</sub> H <sub>82</sub> O <sub>13</sub> N <sub>20</sub> I	C <sub>62</sub> H <sub>82</sub> O <sub>13</sub> N <sub>20</sub> I	C <sub>63</sub> H <sub>84</sub> O <sub>13</sub> N <sub>20</sub> I	C <sub>63</sub> H <sub>84</sub> O <sub>13</sub> N <sub>20</sub> I	C <sub>64</sub> H <sub>86</sub> O <sub>13</sub> N <sub>20</sub> I
FAB-MS (M + 1)	1441	1441	1455	1455	1469
K <sub>i</sub> <sup>a</sup> (nM)	0.59 ± 0.19 (3)	1.1 ± 0.85 (3)	0.47 ± 0.1 (7)	0.27 (2)	0.18 ± 0.06 (3)
K <sub>d</sub> (nM)	0.15 (1)	ND	0.19 ± 0.06 (3)	0.054 ± 0.02 (3)	0.04 ± 0.03 (6)
K <sub>i</sub> <sup>b</sup> (nM)	8 (2)	10 (2)	1.6 (2)	16 (2)	3 (2)
K <sub>i</sub> <sup>c</sup> (nM)	4.8 ± 1.6 (4)	0.65 (2)	37.7 ± 14 (4)	1.4 (2)	18 (2)
K <sub>i act</sub> <sup>c</sup> (nM)	0.20 ± 0.1 (4)	0.24 ± 0.6 (6)	0.11 ± 0.01 (5)	0.13 ± 0.4 (6)	0.46 ± 0.4 (4)
covalent yield <sup>d</sup> (%)	10	15	20	21	

<sup>a</sup> K<sub>i</sub>: inhibition constants determined from competitive binding experiments performed on (a) rat liver membranes (V<sub>1a</sub> receptor subtype), (b) rat kidney membranes (V<sub>2</sub> receptor subtype), and (c) rat mammary glands (OT receptor). The results are the mean values of triplicate determination obtained from the number of experiments indicated in parentheses. <sup>b</sup> K<sub>d</sub>: dissociation constant determined from concentration-dependent binding experiments performed on rat liver membranes (V<sub>1a</sub> receptor subtype). <sup>c</sup> K<sub>i act</sub>: inhibition constant determined from vasopressin-induced inositol phosphates accumulation performed on WRK<sub>1</sub> cell line (V<sub>1a</sub> receptor subtype). <sup>d</sup> The covalent binding yield was determined on rat hepatic V<sub>1a</sub> vasopressin receptor subtype using the filters method.

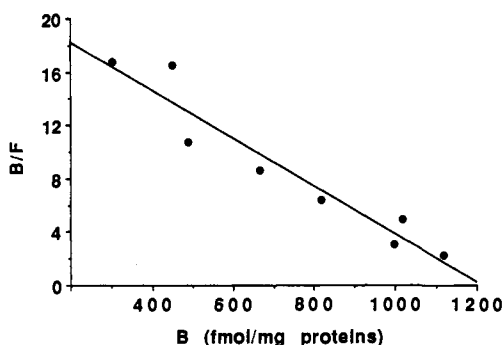


**Figure 4.** Scatchard representation of concentration-dependent binding experiment performed with the iodinated analogue 21. Rat liver membranes (5 μg) were incubated with an increasing concentration of <sup>125</sup>I-labeled analogue 21 (F). Specific binding (B) was calculated as the difference between total and nonspecific binding determined in the presence of a 250-fold excess of the corresponding nonradioactive analogue. The results are the mean of triplicate values and are representative of three independent experiments.

appears that the selectivity of our analogues for one receptor subtype over another is dependent on both the alkyl chain length and the position of the azido group. Moreover, it seems that the influence due to the position of the azido group increases with the alkyl chain length.

**Biological Activities of the Vasopressin Analogues.** We used a biochemical test to determine the agonist or antagonist properties of the vasopressin analogues based on the ability of vasopressin agonists to stimulate inositol phosphates accumulation in WRK<sub>1</sub> cells, a tumor cell line exhibiting high amounts of V<sub>1a</sub> vasopressin receptors tightly coupled with phospholipase C.<sup>22</sup> As it is shown in Figure 5 (panel a), up to 10<sup>-6</sup> M, all analogues tested were unable to stimulate inositol phosphates accumulation. Thus, they were devoid of any intrinsic agonist activities. Yet, they fully antagonized the vasopressin-stimulated inositol phosphates accumulation (Figure 5, panel b). Inhibition constants of vasopressin-stimulated inositol phosphates accumulation (K<sub>i act</sub>) could be determined from these experiments (see the methods). Statistical values obtained for the analogues tested are summarized in Table 3. A rather good correlation was observed between the K<sub>i act</sub> and K<sub>i</sub> of each analogue tested. Such results validated the biological test used to determine the antagonist properties of the analogues.

### Determination of the Covalent Binding Yield.

Preliminary covalent binding yields of the probe-receptor complexes were determined from experiments performed on filters as previously described by Bochet *et al.*<sup>23</sup> Table 3 shows covalent binding yields of analogues 18–21, ranging from 10 to 20%, which are significantly higher than any previously published results (1–2%). Increasing the number of methylene units (n = 0, 1, 2, or 3) between the arylazido group and the D-Tyr<sup>2</sup>(Me) residue improves the affinity of the analogues for the V<sub>1a</sub> vasopressin receptor. This confirms the existence of a receptor domain that tightly binds bulky hydrophobic moieties. This situation is particularly favorable to the formation of covalent bonds.

### Conclusion

We propose a new series of photoreactive and radioiodinatable probes to study vasopressin receptors. Most of our analogues exhibit a high affinity for vasopressin receptors, a rather good selectivity for the V<sub>1a</sub> vasopressin receptor subtype, and antagonistic properties. Moreover, they were able to establish covalent bonds with the vasopressin receptor in unprecedented high yields and were susceptible to iodination without loss of affinity. Therefore, they are very promising molecules for use in the determination of the biochemical properties of the receptor (e.g. molecular weight, glycosylation, and hydrodynamic properties) as for the complete mapping of the receptor binding site. Since the affinity is still increasing with the three-methylene-unit derivative, we are currently designing new probes containing longer chains.<sup>24</sup>

### Experimental Section

**General.** Protected L-amino acids, Boc-D-Tyr(Me)-OH, and p-MBHA resin were purchased from either Propeptide, Novabiochem, or Bachem, and PyBOP was obtained from Novabiochem. Solid-phase peptide synthesis was performed using a manual device as previously described<sup>25</sup> and used analytical-grade solvents. The pH of organic solutions during solid-phase and segment couplings was checked using moistened pH indicator paper. Peptide-resins were deprotected on a Protein Research Foundation Kel-F apparatus using HF obtained from Matheson. UV spectroscopy grade DMF and Me<sub>2</sub>SO were used for the coupling of the (azidophenyl)alkyl acids to peptides. [<sup>3</sup>H]<sub>8</sub>AVP was purchased from Dupont NEN. d(CH<sub>2</sub>)<sub>5</sub>[Tyr(Me)<sup>2</sup>, Thr<sup>4</sup>, Orn<sup>8</sup>, Tyr-NH<sub>2</sub><sup>9</sup>]VT and Phaa-D-Tyr(Me)-Phe-Gln-Asn-Arg-Pro-Arg-Tyr-NH<sub>2</sub> were generously provided by Dr. Manning. All diazo and azido peptide derivatives were handled in dim light.

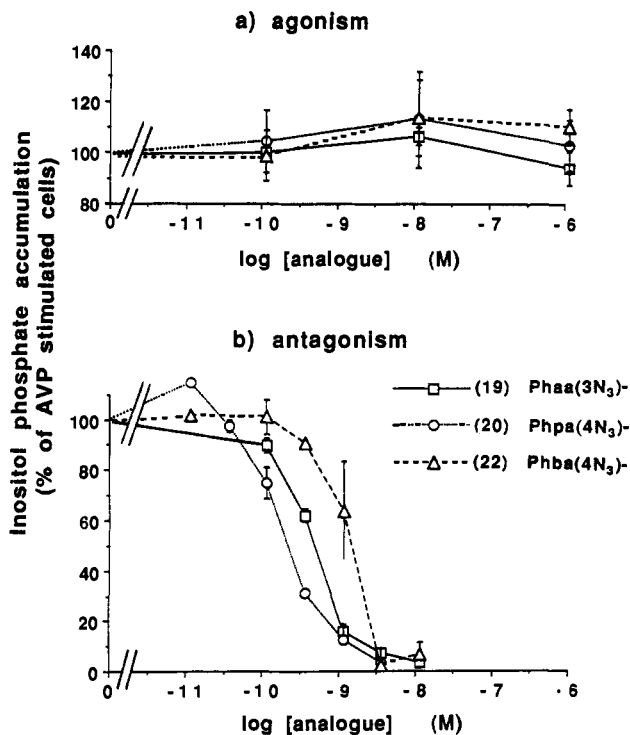


**Figure 5.** Determination of the agonism/antagonism properties of compounds 18–22. Panel a: *myo*-[<sup>3</sup>H]inositol-prelabeled WRK<sub>1</sub> cells were incubated for 21 min at 37 °C in PBS LiCl medium with or without (control) increasing amounts of vasopressin analogues. Total inositol phosphates accumulation was measured as described in the methods. The results are expressed as percent of control (100% =  $1.34 \times 10^4 \pm 1500$  dpm/ $10^6$  cells). Panel b: *myo*-[<sup>3</sup>H]inositol-prelabeled WRK<sub>1</sub> cells were preincubated for 15 min at 37 °C in PBS LiCl medium with or without (control) increasing amounts of vasopressin analogues. AVP (3 nM) (VP-stimulated) or vehicle (basal) was added to the incubation medium for an additional 6-min period. Total inositol phosphates accumulation was determined. The results are expressed as percent of vasopressin response of control cells (VP-stimulated – basal response) (100% =  $6.2 \times 10^4 \pm 1.1 \times 10^4$  dpm/ $10^6$  cells). The inhibition constant  $K_{i \text{ act}}$  of each analogue was calculated as  $K_{i \text{ act}} = \text{IC}_{50} [1 + [\text{AVP}]/K_{\text{act}}]$ , where  $[\text{AVP}] = 3$  nM and  $K_{\text{act}}$  is the concentration of AVP which evokes half-maximal stimulation of total inositol phosphates accumulation.  $K_{\text{act}} = 2.4 \pm 1.0$  nM in these experimental conditions (see reference for details). Since all analogues exhibit a similar profile, only three of them are described for the clarity of the figure. Results are the mean  $\pm$  SE of at least three distinct experiments, each performed in duplicate. When no error bar is shown, it is comprised within the symbols.

**HPLC.** Analytical HPLC was performed on a Shimadzu LC-9A instrument fitted with a Merck Lichrosorb C<sub>18</sub> column (5- $\mu$ m particle size, 4  $\times$  250 mm) and linked to two Waters 440 and 441 detectors operating at 254 and 214 nm, respectively. This instrument was operated using mobile phases of 0.1% TFA/H<sub>2</sub>O (v/v) and 0.1% TFA/CH<sub>3</sub>CN (v/v) with a linear elution gradient of 1% CH<sub>3</sub>CN/min (or stated otherwise) at a flow rate of 2 mL/min (void volume,  $v_0 \approx 1.7$  mL). For analytical HPLC data, the values reported as percent elution correspond to the percent CH<sub>3</sub>CN composition of the eluent passing through the detector cell at the time of UV detection (corrected for  $v_0$ ) since this is more informative than the retention times. Preparative HPLC was performed on a high-pressure Waters 6000A dual pump system equipped with a 720 controller and fitted with a Whatman Partisil ODS 3 Magnum 20 column (10- $\mu$ m particle size, 22  $\times$  500 mm) and linked to both a Waters 440 detector (254 nm) and a Cecil CE 2012 detector (214 nm) ( $v_0 \approx 120$  mL). Peptide purifications were performed using a linear elution gradient (given in each case) at a flow rate of 10 mL/min with elution fractions collected using a Pharmacia Frac 100 collector operating in the peak detection mode.

**NMR.** <sup>1</sup>H NMR spectra were recorded on a AMX 360 Bruker spectrometer operating at 360 MHz and at 305 K. Chemical shifts are referenced to internal [<sup>2</sup>H<sub>5</sub>]Me<sub>2</sub>SO with the residual signal set to 2.50 ppm. All spin systems were identified and assigned by TOCSY, for scalar couplings,<sup>17</sup> and NOESY, for dipolar couplings experiments.<sup>26</sup> Assignments were made using sequential NOEs, mainly between the  $\alpha$  proton of residue *i* with the amide proton of the residue *i* + 1.<sup>23</sup> The NOESY experiment was performed in the time-proportional phase incrementation scheme as described by Marion and Wüthrich<sup>27</sup> with a mixing time of 300 ms. The acquisition of 2D data was performed using 2048 data points and 512 increments followed by computation of the NMR data sets on a Bruker X32 station using the UXNMR program. Time domain data matrices were multiplied by a sinebell function shifted by  $\pi/16$  and  $\pi/8$  in the  $t_2$  and  $t_1$  dimensions, respectively, before Fourier transformation.

**Radioiodination.** Iodogen (15  $\mu$ g) was dissolved in CHCl<sub>3</sub> (100  $\mu$ L) in a 750- $\mu$ L vessel (Eppendorf), and then stood in a fume hood overnight to allow slow solvent evaporation. After successive addition of an aqueous solution of 1 M KH<sub>2</sub>PO<sub>4</sub> buffer (55  $\mu$ L, pH 6.5) and 1 mM azido-peptide (40  $\mu$ L) to the Iodogen-coated vessel, Na<sup>125</sup>I (1 mCi, Amersham, 2200 Ci/mmol) was then added and the vessel agitated (Vortex) and let for 2.5 min at room temperature. The solution was then removed from the vessel and diluted by adding a solution of 0.1% TFA/H<sub>2</sub>O (400  $\mu$ L). The total volume was then immediately applied to a C<sub>18</sub> HPLC column ( $\mu$ Bondapak, particle size 10  $\mu$ m, 3.9  $\times$  300 mm) and eluted with a linear gradient of 0–60% CH<sub>3</sub>CN at a flow rate of 1 mL/min. Fractions were collected every minute and the relative radioactivity was measured by  $\gamma$ -counting. The same HPLC protocol was repeated for a second purification. The procedure was performed using a large excess (100-fold) of peptide over Na<sup>125</sup>I to prevent diiodination. The final HPLC purified radioiodinated compounds 18–22 were stored in liquid nitrogen.

**Membranes Preparation.** Wistar male or female rats (150–200 g) were purchased from Iffa Credo (Lyon, France). Two lots of rat liver membranes (male rat) were prepared according to the method described by Neville<sup>19</sup> up to step 11 and stored in liquid nitrogen (15–20-month-old sample, 7.0 mg of proteins/mL, and 1–3-month-old sample, 7.6 mg of proteins/mL). Rat renal medullary membranes<sup>20</sup> (male rat, 1.96 mg/mL) and rat mammary gland membranes<sup>21</sup> (female rat, 27 mg of proteins/mL) were prepared as previously described and used immediately or stored in liquid nitrogen, respectively.

**Concentration-Dependent Binding Experiments (Competition).** Rat liver membranes (5 or 10  $\mu$ g/assay) were incubated (45 min, 30 °C) in a final volume of 200  $\mu$ L of the following incubation medium: 50 mM Tris-HCl (pH 7.4), 5 mM MgCl<sub>2</sub>, 1 mg/mL BSA, a concentration range for each of the unlabeled azido-peptide ( $10^{-6}$  or  $10^{-7}$  to  $10^{-11}$  M) and a pertinent fixed concentration ( $60 \times 10^{-12}$  M) of [<sup>125</sup>I]Phaa-D-Tyr(Me)-Phe-Gln-Asn-Arg-Pro-Arg-Tyr-NH<sub>2</sub> (Manning's Linear AVP antagonist). Nonspecific binding was determined in the presence of 1  $\mu$ M vasopressin. Reaction was stopped by adding a ice-cold washing solution (5 mL) of 10 mM Tris-HCl (pH 7.4) and 1 mM MgCl<sub>2</sub>. Unbound azido-peptide was eliminated by filtration over Whatman GF/C filters which had been previously soaked in 10 mg/mL BSA for more than 2 h. Filters were then rinsed three times (3  $\pm$  5 mL) with the washing solution, and the radioactivity retained was measured. Binding assays on rat mammary gland (2 or 5  $\mu$ g/assay) and on kidney medulla membranes (28.5  $\mu$ g/assay) were performed using the same protocol but using  $60 \times 10^{-12}$  M [<sup>125</sup>I]d(CH<sub>2</sub>)<sub>5</sub>[Tyr(Me)<sup>2</sup>, Thr<sup>4</sup>, Orn<sup>8</sup>, Tyr-NH<sub>2</sub><sup>9</sup>]VT and  $10^{-9}$  M [<sup>3</sup>H]AVP, respectively. Nonspecific binding were determined in the presence of 1  $\mu$ M oxytocin for assays on rat mammary glands membranes and of 1  $\mu$ M vasopressin for those on kidney membranes.

**Concentration-Dependent Binding Experiments.** These experiments were performed according to the protocol described above and with appropriate amounts of radioiodinated analogues. Nonspecific binding was determined in the presence of an excess of the corresponding unlabeled analogue.

**WRK<sub>1</sub> Cell Culture.** WRK<sub>1</sub> cells were established and grown as previously described.<sup>28</sup> Briefly, cells were plated in a 3.5-cm plastic dishes at a density of  $5 \times 10^4$  to  $7 \times 10^4$  cells in minimum essential medium containing Earle's salt, 5% fetal calf serum

(v/v), 2% decomplexed rat serum (v/v), 2 mM glutamine, 100 units/mL penicillin, and 100 mg/mL streptomycin. The medium was changed after 2 days and replaced by a similar culture medium enriched in *m*-yo-[<sup>3</sup>H]inositol (2  $\mu$ Ci/mL). Experiments were performed 3 days later.

**Determination of Inositol Phosphates Accumulation.** Experiments were performed as previously described.<sup>29</sup> Briefly, the culture medium was discarded, and the cells were incubated for 30 min in the same medium without sera and tritiated inositol. Cells were then washed two times with phosphate-buffered saline medium (PBS) (see ref 29 for composition) and further incubated for 15 min at 37 °C in PBS medium containing 10 mM LiCl, 1 mg/mL BSA, and various concentrations of analogues. Basal or stimulated accumulation of inositol phosphates was determined after a 6-min incubation period at 37 °C. The reaction was stopped by adding perchloric acid (5% v/v final concentration). The cells were scraped off and the resulted extracts neutralized with Hepes-KOH. Accumulated inositol phosphates were separated by batch elution on Dowex columns (IX-10, 200-400 mesh, formate form) as earlier described.<sup>29</sup> Previous studies on these cells demonstrated that vasopressin and agonists stimulated the accumulation of inositol phosphates in a time- and concentration-dependent manner.<sup>29,30</sup> As the concentrations of vasopressin analogues leading to half maximum stimulation of InsP<sub>1</sub>, InsP<sub>2</sub>, and InsP<sub>3</sub> accumulation were similar, whatever the inositol phosphate isomer, we have measured the bulk concentration of inositol phosphates.<sup>22</sup>

**UV Photolabeling of the Ligand-Receptor Complex.** The photolabeling of the ligand-receptor complexes was performed as previously described.<sup>23</sup> The procedure was identical to that used in the binding experiments except that BSA was omitted from both the incubation buffer and the soaking solution in order to avoid its photolabeling. Once rinsed, the filters were rapidly laid on an ice-cold surface and irradiated for 10 min at 10 cm under five Philips TUV6 lamps (254 nm). The proteins were then solubilized from the filters in 1 mL of the following medium: 50 mM Tris-HCl, 2% SDS, and 1 mM EDTA (pH 7.4). After one night of solubilization, the filters were rinsed twice with water (1 mL) and eliminated. Water (1 mL) and 10 mg/mL BSA (40  $\mu$ L) were successively added to the solubilized samples and the proteins then precipitated with 72% trichloroacetic acid (0.8 mL) for 4 h at 4 °C. The samples were centrifuged in a Jouan CR1000 at 4000g for 30 min at 4 °C. The supernatant was then eliminated and the radioactivity remaining in the pellets was measured. Two sets of experiments were performed, one being irradiated while the other one was kept in dim light (negative control). The covalent binding yield was expressed as the ratio between the specific binding measured from the irradiated membranes ( $B_{0\text{ir}}$ ) and the specific binding measured from a set of BSA-soaked filters ( $B_{0\text{as}}$  as determined in binding experiments). Covalent yield =  $100 \times (B_{0\text{ir}}/B_{0\text{as}})$  (Table 3).

**Synthesis of the Octapeptide Segment: H-D-Tyr(Me)-Phe-Gln-Asn-Arg-Pro-Arg-Tyr-NH<sub>2</sub>-3TFA (1).** Solid-phase synthesis of octapeptide 1 was performed using 4-methylbenzhydrylamine (*p*-MBHA) resin (2 g with 0.8 mmol/g of titratable amine, 1.6 mmol) and Boc-protected amino acids (2 equiv) using the following side-chain protections: Tyr(Dcb), Arg(Tos), Asn(Xan), and Gln(Xan). The couplings were performed using PyBOP (2 equiv, similar protocol as for BOP<sup>25</sup>), the Boc-amino acid (2 equiv), and a sufficient quantity of DIEA (generally >5 equiv) to maintain the pH around 7-8. DMF and DCM were essentially used as the coupling solvents, and the efficiency of each coupling was monitored by the qualitative ninhydrin test.<sup>31</sup> As the coupling of Boc-Asn-OH was incomplete, this residue was recoupled using Boc-Asn(Xan)-OH in DMF. The Boc group was removed after each coupling by the use of TFA/DCM/dithioethanol (50:47:3, v/v). Deprotection of a portion of the octapeptidyl resin (0.7 g from the 5.35 g obtained) by HF/anisole (9:1, v/v; 9 mL) at 0 °C, gave 0.29 g of crude product after lyophilization. HPLC purification of 0.22 g (five runs) gave the octapeptide-TFA (1) (0.12 g) as a white fluffy solid. Its structure was ascertained by <sup>1</sup>H NMR (Table 1). HPLC gradient: 0-50% CH<sub>3</sub>CN over 25 min. CH<sub>3</sub>CN elution: 27%;  $\epsilon_{214}/\epsilon_{254} = 37$ . Preparative HPLC gradient: 0-17, 17-27, 27, 27-50% CH<sub>3</sub>CN over 5, 50, 10, and 5 min, respectively.

**Bz(4-NH<sub>2</sub>)-D-Tyr(Me)-Phe-Gln-Asn-Arg-Pro-Arg-Tyr-NH<sub>2</sub>-3TFA (2).** Octapeptide-resin (0.80 g) was coupled with 4-aminobenzoic acid (Fluka, 0.1 g, 0.7 mmol). HF deprotection (10 mL) of the peptide-resin gave 0.32 g of crude product 2. Analytical HPLC gradient: 0-50%. CH<sub>3</sub>CN elution: 30.5%;  $\epsilon_{214}/\epsilon_{254} = 6.4$ .

**Bz(4-N<sub>3</sub>)-D-Tyr(Me)-Phe-Gln-Asn-Arg-Pro-Arg-Tyr-NH<sub>2</sub>-2TFA (3).** Peptide 2 (50 mg, 39  $\mu$ mol) was dissolved in 0.1 M HCl (5 mL) at 0 °C. A solution of 1 M NaNO<sub>2</sub> (41  $\mu$ L, 1.05 equiv) was added and the diazotization was performed at 0 °C for 15 min, in the dark, under HPLC monitoring (% elution of the N<sub>2</sub><sup>+</sup> intermediate: 29). As a first addition of 1 M NaN<sub>3</sub> (43  $\mu$ L, 1.1 equiv) gave an incomplete azide substitution, a further solution of NaN<sub>3</sub> (20  $\mu$ L, 0.5 equiv) was added and the reaction mixture stirred at room temperature. HPLC purification gave peptide 3 as a white fluffy solid (21 mg, 35% recovery). HPLC gradient: 0-50% CH<sub>3</sub>CN over 25 min. CH<sub>3</sub>CN elution: 39%;  $\epsilon_{214}/\epsilon_{254} = 3.7$ . Preparative HPLC gradient: 0-32, 32-42, 42, 42-50% CH<sub>3</sub>CN over 10, 50, 10, and 5 min, respectively.

**General Procedure for the Synthesis of (Azidophenyl)alkyl Acid Derivatives (4, 5, 6, 8, 10).** A solution of 1 M NaNO<sub>2</sub> (1.1 equiv) was added to a solution of (aminophenyl)alkyl acid (1 equiv) in 2 M HCl and the diazotization performed for 15 min at 0 °C, in the dark. A solution of 1 M NaN<sub>3</sub> (1.05 equiv) was then added and the reaction mixture was stirred for 90 min. The precipitated solid was collected by filtration, rinsed with water (50 mL), and then dried under vacuum. The filtrate was further extracted with AcOEt, the organic phase dried on MgSO<sub>4</sub>, and the solvent evaporated *in vacuo*.<sup>15</sup>

**3-Azidobenzoic Acid {Bz(3-N<sub>3</sub>)-OH} (4).** The reaction was performed according to the general procedure, using 3-aminobenzoic acid (Aldrich, 1 g, 7.3 mmol), and gave compound 4 as a off-white amorphous solid (1.11 g, 96%). HPLC gradient: 0-40%. CH<sub>3</sub>CN elution: 27%;  $\epsilon_{214}/\epsilon_{254} = 1.0$ .

**4-Azidophenylacetic Acid {Phaa(4-N<sub>3</sub>)-OH} (5).** The reaction was performed using 4-aminophenylacetic acid (Fluka, 0.5 g, 3.31 mmol) and gave the crude compound 5 as a pink amorphous solid (0.464 g, 80%). HPLC gradient: 0-40%. CH<sub>3</sub>CN elution: 31%;  $\epsilon_{214}/\epsilon_{254} = 0.5$ .

**3-Azidophenylacetic Acid {Phaa(3-N<sub>3</sub>)-OH} (6).** The reaction was performed using 3-aminophenylacetic acid (Aldrich, 0.20 g, 1.33 mmol) and gave compound 6 as a cream amorphous solid (0.224 g, 95%). HPLC gradient: 0-40%. CH<sub>3</sub>CN elution: 29.5%;  $\epsilon_{214}/\epsilon_{254} = 1.2$ .

**3-(4-Aminophenyl)propionic Acid {Phpa(4-NH<sub>2</sub>)-OH} (7).** Hydrogen was slowly bubbled into a stirred solution of 4-aminocinnamic acid (Aldrich, 1.0 g, 6.13 mmol) in AcOH/MeOH (25%, 70 mL) containing 10% Pd/C (120 mg). After reaction overnight, the catalyst was removed by filtration on Celite and the solvent evaporated *in vacuo* to give the crude compound 7 as a pink-orange solid (5.75 mmol, 94%). HPLC gradient: 0-35%. CH<sub>3</sub>CN elution: 7.5%;  $\epsilon_{214}/\epsilon_{254} = 14.7$ .

**3-(4-Azidophenyl)propionic Acid {Phpa(4-N<sub>3</sub>)-OH} (8).** The reaction was performed according to the general azidation procedure using compound 7 (400 mg, 2.43 mmol) and gave the crude compound 8 as a yellow amorphous solid (350 mg, 75%). HPLC gradient: 0-35%. CH<sub>3</sub>CN elution: 33%;  $\epsilon_{214}/\epsilon_{254} = 0.6$ .

**3-(3-Aminophenyl)propionic Acid {Phpa(3-NH<sub>2</sub>)-OH} (9).** Hydrogen was slowly bubbled into a stirred solution of 3-nitrocinnamic acid (Aldrich, 500 mg, 2.6 mmol) in AcOH/MeOH (25%, 100 mL) containing 10% Pd/C (0.2 g). After reaction for 30 min, the catalyst was removed by filtration on Celite and the solvent evaporated *in vacuo* to give compound 9 as a gray solid (0.36 g, 84%). HPLC gradient: 0-40%. CH<sub>3</sub>CN elution: 8%;  $\epsilon_{214}/\epsilon_{254} = 33$ .

**3-(3-Azidophenyl)propionic Acid {Phpa(3-N<sub>3</sub>)-OH} (10).** The reaction was performed according to the general azidation procedure using compound 9 (200 mg, 1.21 mmol) and gave the crude compound 10 as an amorphous pink-brown solid (130 mg, 56%). HPLC gradient: 0-40%. CH<sub>3</sub>CN elution: 32%;  $\epsilon_{214}/\epsilon_{254} = 1.4$ .

**4-(4-Azidophenyl)butyric Acid {Phba(4-N<sub>3</sub>)-OH} (11).** The reaction was performed according to the general azidation procedure using 4-(4-aminophenyl)butyric acid (Aldrich, 500 mg, 2.8 mmol) and gave compound 11 as an amorphous white solid

(485 mg, 85%). HPLC gradient: 0–60%. CH<sub>3</sub>CN elution: 45.5%;  $\epsilon_{214}/\epsilon_{254} = 0.66$ .

**General Procedure for PyBOP Coupling of an (Azidophenyl)alkyl Acid to the Octapeptide 1.** To a stirred solution of pure octapeptide 1 (in 200  $\mu$ L of UV-grade Me<sub>2</sub>SO) were added (azidophenyl)alkyl acid (2.5 equiv) and PyBOP (2.5 equiv) at room temperature in the dark. DIEA (5 equiv) was added progressively and monitoring of the coupling showed it was complete after 1 h. The target compound was identified as the major formed peak from its pertinent UV properties ( $\epsilon_{214}/\epsilon_{254}$ ).<sup>16</sup> The total volume was then applied to the preparative C<sub>18</sub> HPLC column and eluted using a linear gradient of CH<sub>3</sub>CN (0.2%/min). The fraction corresponding to the expected compound was collected and lyophilized to give the pure azidopeptide as a white fluffy solid.

**Bz(3-N<sub>3</sub>)-D-Tyr(Me)-Phe-Gln-Asn-Arg-Pro-Arg-Tyr-NH<sub>2</sub>-2TFA** {[Bz(3-N<sub>3</sub>)<sup>1</sup>,D-Tyr(Me)<sup>2</sup>,Arg<sup>6</sup>,Tyr<sup>9</sup>]AVP} (12). The reaction was performed according to the general coupling procedure with peptide 1 (10 mg, 7  $\mu$ mol) and compound 4 to give peptide 12 as a white fluffy solid (8 mg, 75% recovery). HPLC gradient: 0–40%. CH<sub>3</sub>CN elution: 37%;  $\epsilon_{214}/\epsilon_{254} = 3.2$ . Preparative HPLC gradient: 0–20, 20–40, and 40–60% CH<sub>3</sub>CN over 10, 50, and 20 min, respectively.

**Phaa(4-N<sub>3</sub>)-D-Tyr(Me)-Phe-Gln-Asn-Arg-Pro-Arg-Tyr-NH<sub>2</sub>-2TFA** {[Phaa(4-N<sub>3</sub>)<sup>1</sup>,D-Tyr(Me)<sup>2</sup>,Arg<sup>6</sup>,Tyr<sup>9</sup>]AVP} (13). The reaction was performed with peptide 1 (10 mg, 7  $\mu$ mol) and compound 5 to give peptide 13 as a white fluffy solid (8 mg, 74% recovery). HPLC gradient: 0–60%. CH<sub>3</sub>CN elution: 38%;  $\epsilon_{214}/\epsilon_{254} = 2.6$ . Preparative HPLC gradient: 0–30 and 30–50% CH<sub>3</sub>CN over 50 and 20 min, respectively.

**Phaa(3-N<sub>3</sub>)-D-Tyr(Me)-Phe-Gln-Asn-Arg-Pro-Arg-Tyr-NH<sub>2</sub>-2TFA** {[Phaa(3-N<sub>3</sub>)<sup>1</sup>,D-Tyr(Me)<sup>2</sup>,Arg<sup>6</sup>,Tyr<sup>9</sup>]AVP} (14). The reaction was performed with peptide 1 (10 mg, 7  $\mu$ mol) and compound 6 to give peptide 14 as a white fluffy solid (10 mg, 93% recovery). HPLC gradient: 0–60%. CH<sub>3</sub>CN elution: 38%;  $\epsilon_{214}/\epsilon_{254} = 3.9$ . Preparative HPLC gradient: 0–20, 20–40, and 40–60% CH<sub>3</sub>CN over 10, 50, and 20 min, respectively.

**Phpa(4-N<sub>3</sub>)-D-Tyr(Me)-Phe-Gln-Asn-Arg-Pro-Arg-Tyr-NH<sub>2</sub>-2TFA** {[Phpa(4-N<sub>3</sub>)<sup>1</sup>,D-Tyr(Me)<sup>2</sup>,Arg<sup>6</sup>,Tyr<sup>9</sup>]AVP} (15). The reaction was performed with peptide 1 (10 mg, 7  $\mu$ mol) and compound 8 to give peptide 15 as a white fluffy solid (8.5 mg, 78% recovery). HPLC gradient: 0–60%. CH<sub>3</sub>CN elution: 39%;  $\epsilon_{214}/\epsilon_{254} = 2.5$ . Preparative HPLC gradient: 0–20, 20–40, and 40–60% CH<sub>3</sub>CN over 10, 50, and 20 min, respectively.

**Phpa(3-N<sub>3</sub>)-D-Tyr(Me)-Phe-Gln-Asn-Arg-Pro-Arg-Tyr-NH<sub>2</sub>-2TFA** {[Phpa(3-N<sub>3</sub>)<sup>1</sup>,D-Tyr(Me)<sup>2</sup>,Arg<sup>6</sup>,Tyr<sup>9</sup>]AVP} (16). The reaction was performed with peptide 1 (10 mg, 7  $\mu$ mol) and compound 10 to give derivative 16 as a white fluffy solid (6.5 mg, 60% recovery). HPLC gradient: 0–60%. CH<sub>3</sub>CN elution: 40%;  $\epsilon_{214}/\epsilon_{254} = 4.4$ . Preparative HPLC gradient: 0–20, 20–40, and 40–60% CH<sub>3</sub>CN over 10, 50, and 20 min, respectively.

**Phba(4-N<sub>3</sub>)-D-Tyr(Me)-Phe-Gln-Asn-Arg-Pro-Arg-Tyr-NH<sub>2</sub>-2TFA** {[Phba(4-N<sub>3</sub>)<sup>1</sup>,D-Tyr(Me)<sup>2</sup>,Arg<sup>6</sup>,Tyr<sup>9</sup>]AVP} (17). The reaction was performed with peptide 1 (10 mg, 7  $\mu$ mol) and compound 11 to give derivative 17 as a white fluffy solid (7.0 mg, 60% recovery). HPLC gradient 0–60%. CH<sub>3</sub>CN elution: 45%;  $\epsilon_{214}/\epsilon_{254} = 2.4$ . Preparative HPLC gradient: 0–30 and 30–60% CH<sub>3</sub>CN over 10 and 60 min, respectively.

**General Procedure for the ICl Iodination of the Azidopeptides.** Peptides were iodinated according to an optimized procedure determined for each run on a reduced quantity by analytical RP-HPLC monitoring, and the reaction was extrapolated to a larger scale for a semipreparative run. Briefly, a 0.01 M ICl solution in MeOH (1.2 mL, 2.3 equiv) was added to a solution of azidopeptide (containing one Tyr, 1 equiv) in MeOH (0.8 mL) and stirred in the dark for 8–10 min at room temperature. The total reaction volume was then applied to the semipreparative C<sub>18</sub> HPLC column and eluted using a linear gradient of 0–30 and 30–50% CH<sub>3</sub>CN over 10 and 50 min, respectively (or stated). The fractions corresponding to the second of the three obtained peaks were collected and lyophilized to give the pure monoiodinated azidopeptide.

**Phaa(4-N<sub>3</sub>)-D-Tyr(Me)-Phe-Gln-Asn-Arg-Pro-Arg-Tyr(3-I)-NH<sub>2</sub>-2TFA** {[Phaa(4N<sub>3</sub>)<sup>1</sup>,D-Tyr(Me)<sup>2</sup>,Arg<sup>6</sup>,Tyr(3-I)<sup>9</sup>]AVP} (18). The reaction was performed according to the general procedure, except that 0.35 mL of 0.01 M ICl (2.7 equiv) was

added to a solution of derivative 13 (2.0 mg, 1.3 mL) to give derivative 18 as a pure white fluffy solid (0.5 mg, 23% recovery). HPLC gradient: 0–60%. CH<sub>3</sub>CN elution of the monoiodinated (I<sub>1</sub>) derivative: 39.5%;  $\epsilon_{214}/\epsilon_{254} = 3.6$ . CH<sub>3</sub>CN elution of the diiodinated (I<sub>2</sub>) derivative: 41.5%;  $\epsilon_{214}/\epsilon_{254} = 3.4$ . Preparative HPLC gradient: 0–35, 35–45, and 45% CH<sub>3</sub>CN over 10, 50, and 5 min, respectively.

**Phaa(3-N<sub>3</sub>)-D-Tyr(Me)-Phe-Gln-Asn-Arg-Pro-Arg-Tyr(3-I)-NH<sub>2</sub>-2TFA** {[Phaa(3-N<sub>3</sub>)<sup>1</sup>,D-Tyr(Me)<sup>2</sup>,Arg<sup>6</sup>,Tyr(3-I)<sup>9</sup>]AVP} (19). The reaction was performed using derivative 14 (8 mg, 5.2  $\mu$ mol) to give compound 19 as a pure white fluffy solid (2.3 mg, 26% recovery). HPLC gradient 20–50%. CH<sub>3</sub>CN elution: 43%;  $\epsilon_{214}/\epsilon_{254} = 5.0$ . CH<sub>3</sub>CN elution of the diiodinated derivative: 45%;  $\epsilon_{214}/\epsilon_{254} = 5.2$ .

**Phpa(4-N<sub>3</sub>)-D-Tyr(Me)-Phe-Gln-Asn-Arg-Pro-Arg-Tyr(3-I)-NH<sub>2</sub>-2TFA** {[Phpa(4-N<sub>3</sub>)<sup>1</sup>,D-Tyr(Me)<sup>2</sup>,Arg<sup>6</sup>,Tyr(3-I)<sup>9</sup>]AVP} (20). The reaction was performed using derivative 15 (8 mg, 5.1  $\mu$ mol) to give compound 20 as a pure white fluffy solid (2.7 mg, 31% recovery). HPLC gradient: 20–50%. CH<sub>3</sub>CN elution: 45%;  $\epsilon_{214}/\epsilon_{254} = 3.4$ . CH<sub>3</sub>CN elution of the diiodinated derivative: 47%;  $\epsilon_{214}/\epsilon_{254} = 3.4$ .

**Phpa(3-N<sub>3</sub>)-D-Tyr(Me)-Phe-Gln-Asn-Arg-Pro-Arg-Tyr(3-I)-NH<sub>2</sub>-2TFA** {[Phpa(3-N<sub>3</sub>)<sup>1</sup>,D-Tyr(Me)<sup>2</sup>,Arg<sup>6</sup>,Tyr(3-I)<sup>9</sup>]AVP} (21). The reaction was performed using derivative 16 (8 mg, 5.1  $\mu$ mol) to give compound 21 as a pure white fluffy solid (2.88 mg, 33% recovery). HPLC gradient: 20–50%. CH<sub>3</sub>CN elution: 42.5%;  $\epsilon_{214}/\epsilon_{254} = 5.3$ . CH<sub>3</sub>CN elution of the diiodinated derivative: 44.5%.

**Phba(4-N<sub>3</sub>)-D-Tyr(Me)-Phe-Gln-Asn-Arg-Pro-Arg-Tyr(3-I)-NH<sub>2</sub>-2TFA** {[Phba(4-N<sub>3</sub>)<sup>1</sup>,D-Tyr(Me)<sup>2</sup>,Arg<sup>6</sup>,Tyr(3-I)<sup>9</sup>]AVP} (22). The reaction was performed using derivative 17 (1.6 mg, 1.2  $\mu$ mol) to give compound 22 as a pure white fluffy solid (1.0 mg, 46% recovery). HPLC gradient: 0–60% over 30 min. CH<sub>3</sub>CN elution: 48.0%;  $\epsilon_{214}/\epsilon_{254} = 3.35$ . CH<sub>3</sub>CN elution of the diiodinated derivative: 51.0%.

**Acknowledgment.** This work was supported by the Institut National pour la Santé et la Recherche Médicale, the Centre National pour la Recherche Scientifique, and the Ministère de la Recherche et de la Technologie. The authors are most thankful to Dr. S. Jard for constant interest, Dr. P. Jouin for the provision of laboratory facilities, and Pr. Aubagnac (University of Montpellier) for the provision of FAB-MS determinations. We also thank Dr. J. W. Perich for assistance during the preparation of this manuscript and for useful discussions.

## References

- Manning, M.; Klis, W. A.; Kruszynski, M.; Przybylski, J. P.; Olma, A.; Wo, N. C.; Pelton, G. H.; Sawyer, W. H. Novel linear antagonists of the antidiuretic (V<sub>2</sub>) and vasopressor (V<sub>1</sub>) responses to vasopressin. *Int. J. Pept. Protein Res.* 1988, 32, 455–467.
- Manning, M.; Przybylski, J. P.; Olma, A.; Klis, W. A.; Kruszynski, M.; Wo, N. C.; Pelton, G. H.; Sawyer, W. H. No requirement of cyclic conformation of antagonists in binding to vasopressin receptors. *Nature* 1987, 329, 839–840.
- Schmidt, A.; Audigier, S.; Barberis, C.; Jard, S.; Manning, M.; Kolodziejczyk, A. S.; Sawyer, W. H. A radioiodinated linear vasopressin antagonist: A ligand with high affinity and specificity for V<sub>1a</sub> receptors. *FEBS Lett.* 1991, 282, 77–81.
- Marie, J.; Roy, C. Covalent labeling of vasopressin receptors from LLC-PK<sub>1</sub> cells by the use of a bifunctional reagent. *Mol. Pharmacol.* 1988, 33, 432–440.
- Buku, A.; Gazis, D.; Eggena, P. Photoaffinity, biotinylation, and iodo analogues as probes for vasotocin receptors. *J. Med. Chem.* 1989, 32, 2432–2435.
- Hegyi, G.; Michel, H.; Shabanowitz, J.; Hunt, D. F.; Chatterjee, N.; Healy-Louie, G.; Elzinga, M. Gln-41 is intermolecularly cross-linked to Lys-113 in F-actin by N-(4-azidobenzoyl)-putrescine. *Protein Science* 1992, 1, 132–144.
- Lutz, W. H.; Londowski, J. M.; Kumar, R. Synthesis and biological activity of a biotinylated vasopressin analog. *Peptides* 1990, 11, 687–691.
- Lutz, W. H.; Londowski, J. M.; Kumar, R. The synthesis and biological activity of four novel fluorescent vasopressin analogs. *J. Biol. Chem.* 1990, 265, 4657–4663.
- Barbeau, D.; Guay, S.; Neugebauer, W.; Escher, E. Preparation and biological activities of potential vasopressin photoaffinity labels. *J. Med. Chem.* 1992, 35, 151–157.



- (10) Bothner-By, A. A.; Lemarie, B.; Walter, R.; Co, R.; Rabbani, L. D.; Breslow, E. NMR and equilibrium dialysis studies of the interaction of bovine neurophysin-I with vasopressin and small peptides. *Int. J. Pept. Protein Res.* 1980, 16, 450-463.
- (11) Manning, M.; Bankowski, K.; Barberis, C.; Jard, S.; Elands, J.; Chan, W. Y. Novel approach to the design of synthetic radioiodinated linear V<sub>1A</sub> receptor antagonists of vasopressin. *Int. J. Pept. Protein Res.* 1992, 40, 261-267.
- (12) Lutz, W.; Londowski, J. M.; Sanders, M.; Salisbury, J.; Kumar, R. A vasopressin analog that binds but does not activate V<sub>1</sub> or V<sub>2</sub> vasopressin receptors is not internalized into cells that express V<sub>1</sub> or V<sub>2</sub> receptors. *J. Biol. Chem.* 1992, 267, 1109-1115.
- (13) Lutz, W.; Sanders, M.; Salisbury, J.; Kumar, R. Internalization of vasopressin analogs in kidney and smooth muscle cells: evidence for receptor-mediated endocytosis in cells with V<sub>2</sub> or V<sub>2</sub> receptors. *Proc. Natl. Acad. Sci. U.S.A.* 1990, 6507-6411.
- (14) Coste, J.; Le-Nguyen, D.; Castro, B. PyBOP: A new coupling reagent devoid of toxic by-product. *Tetrahedron Lett.* 1990, 31, 205-208.
- (15) Dolence, E. K.; Morita, H.; Watt, D. S. Utilization of a nitrenium ion cyclization in a synthesis of a photoreactive prostaglandin, 17-(4-azido-2-hydroxyphenyl)-18,19,20-trinorprostaglandin F<sub>2α</sub>. *Tetrahedron Lett.* 1987, 28, 43-46.
- (16) Seyer, R.; Aumelas, A. Synthesis of biotinylated and photoreactive probes for angiotensin receptors. *J. Chem. Soc. Perkin Trans. 1* 1990, 3289-3299.
- (17) Davis, D. G.; Bax, A. Assignment of complex <sup>1</sup>H NMR spectra via two-dimensional homonuclear Hartmann-Hahn spectroscopy. *J. Am. Chem. Soc.* 1985, 107, 2821-2822.
- (18) Wüthrich, K. *NMR of Proteins and Nucleic Acids*, J. Wiley & Sons Eds; New York, 1986.
- (19) Neville, D. M. Isolation of an organic specific protein antigen from cell-surface membrane of rat liver. *Biochim. Biophys. Acta* 1968, 154, 540-522.
- (20) Guillon, G.; Couraud, P. O.; Butlen, D.; Cantau, B.; Jard, S. Size of vasopressin receptors from rat liver and kidney. *Eur. J. Biochem.* 1980, 111, 287-294.
- (21) Elands, J.; Barberis, C.; Jard, S. [<sup>3</sup>H][Thr<sup>4</sup>Gly<sup>7</sup>] OT: a highly selective ligand for control and peripheral OT receptors. *Am. J. Physiol.* 1988, 254, E31-E38.
- (22) Guillon, G.; Barbeau, D.; Neugebauer, W.; Guay, S.; Bilodeau, L.; Balestre, M. N.; Gallo-Payet, N.; Escher, E. Fluorescent peptide hormones: development of high affinity vasopressin analogues. *Peptides* 1992, 13, 7-11.
- (23) Bochet, P.; Icard-Liepkalns, C.; Pasquini, F.; Garbay-Jaureguiberry, C.; Beaudet, A.; Roques, B.; Rossier, J. Photoaffinity labeling of opioid δ receptors with an iodinated azido-ligand: [<sup>125</sup>I][D-Thr<sup>2</sup>,pN<sub>3</sub>-Phe<sup>4</sup>,Leu<sup>6</sup>]enkephalyl-Thr<sup>6</sup>. *Mol. Pharmacol.* 1988, 34, 436-443.
- (24) Powers, S. P.; Foo, I.; Pinon, D.; Klueppelberg, U. G.; Hedstrom, J. F.; Miller, L. J. Use of photoaffinity probes containing poly(ethylene glycol) spacers for topographical mapping of the cholecystokinin receptor complex. *Biochemistry* 1991, 30, 676-682.
- (25) Le Nguyen, D.; Heitz, A.; Castro, B. Renin substrates. Part 2. Rapid solid phase synthesis of the ratine sequence tetradecapeptide using BOP reagent. *J. Chem. Soc. Perkin Trans. 1* 1987, 1915-1919.
- (26) Macura, S.; Ernst, R. R. Elucidation of cross relaxation in liquids by two-dimensional NMR spectroscopy. *Mol. Phys.* 1980, 41, 95-117.
- (27) Marion, D. and Wüthrich, K. Application of phase sensitive two-dimensional correlated spectroscopy (COSY) for measurement of <sup>1</sup>H-<sup>1</sup>H spin-spin coupling constants in proteins. *Biochem. Biophys. Res. Commun.* 1983, 113, 967-974.
- (28) Guillon, G.; Kirk, C. J.; Balestre, M. N. Characterization of specific V<sub>1a</sub> vasopressin binding sites on a rat mammary tumor cell line. *Biochem. J.* 1986, 240, 189-196.
- (29) Kirk, C. J.; Guillon, G.; Balestre, M. N.; Jard, S. Stimulation, by vasopressin and other agonists, of inositol-lipid breakdown and inositol phosphate accumulation in WRK<sub>1</sub> cells. *Biochem. J.* 1986, 240, 197-204.
- (30) Mouillac, B.; Balestre, M. N.; Guillon, G. Transient inositol (1,4,5) triphosphate accumulation under vasopressin stimulation in WRK<sub>1</sub> cells: Correlation with intracellular calcium mobilization. *Biochem. Biophys. Res. Commun.* 1989, 159, 953-960.
- (31) Kaiser, E.; Colescott, R. L.; Bossinger, C. D.; Cook, P. I. Color test for detection of free terminal amino groups in the solid-phase synthesis of peptides. *Anal. Biochem.* 1970, 34, 595-598.